

# MISSION ANALYSIS OF HEVELIUS – LUNAR MICROSATELLITE MISSION

**Ettore Scari, Matteo Ceriotti, Camilla Colombo, Massimiliano Vasile**  
Dipartimento di Ingegneria Aerospaziale, Politecnico di Milano  
Via La Masa 34, 20156, Milan, Italy. Email : vasile@aero.polimi.it

### ABSTRACT

This paper describes the mission analysis and design of the “Hevelius - Lunar Microsatellite Mission”. The main goal of the overall mission is to place a net-lander on the far side of the Moon to perform some scientific experiments. Two different satellites have been designed to achieve this objective: a microsatellite orbiter to support the net-lander and a carrier spacecraft to transport the net-lander. An L2 Halo orbit has been selected for the orbiter in order to have a constant communication link between the landers and the Earth. The invariant manifolds of the Earth-Moon system have been used to design a low coast transfer trajectory to the L2 Halo orbit. Prior to the beginning of landing operations the carrier is parked into a frozen orbit after a WSB transfer. Finally the descent and landing phases have been designed in order to accomplish the final goals. The whole mission analysis and design process has been driven by the need for a low cost and low risk mission.

### INTRODUCTION

Since the early post-Apollo period, the idea of missions to the far side of the Moon became attractive. However such kinds of missions (e.g. human/robotic exploration, permanent bases or placement of space telescopes and other scientific packages) would be unable to maintain any contact with the ground stations on Earth.

As outlined by Farquhar and Schmid<sup>1,2,3</sup> an uninterrupted communications link with the Earth could be established by forcing a single relay satellite to follow a trajectory about the Earth-Moon L2 libration point, where it would always be visible from both spots. The first application of libration-point orbits and their associated transfer trajectories was the ISEE-3 spacecraft mission. On November 20, 1978, the ISEE-3 spacecraft was successfully placed on a halo orbit about the Sun-Earth L1 libration point by a direct transfer trajectory<sup>4</sup>.

Since that date other missions to libration points have been successfully designed with an associated great development of studies of the multi-body dynamic<sup>5-15</sup>.

One of practical results was the effective design of low-energy transfers to the Moon; in fact different solutions have shown a saving up to 22% in total  $\Delta v$  cost, though with a sensible increment in the time of flight.

The consequent saving of the required propellant and the technological development in manufacturing miniaturized but capable payload instruments has opened a new frontier in space

mission design based on small-sized and low-cost missions<sup>16</sup>.

Small-size buses substantially reduce mission cost by enabling cheap access to space via piggyback or ride-sharing launch opportunities into high Earth orbit, and a rapid development schedule.

In this scenario the Hevelius - Lunar Microsatellite Mission aims at placing a net lander on the far side of the Moon to perform scientific experiments and to test new key enabling technologies. The mission analysis and design process has been driven by strict low cost and low mass requirements. A great effort has been put in the integration of the payload in the limits of a small bus in order to reduce the launch cost to a minimum.

To satisfy these objectives all the recent technologies and innovative mission analysis concepts has been considered as described in this paper.

### 1 THE MISSION

The objective of the mission is the design of a microsatellite that should operate as an orbiter around the Moon to support a net-lander on the far side.

The high-level mission requirements ask for the design of two kinds of spacecraft: an orbiter and at least three landers. A preliminary trade-off analysis led to the choice of a carrier spacecraft to deliver the net landers on the far side of the Moon. The payloads installed on the different spacecraft are expected to provide:

- scientific knowledge on the properties of the lunar soil. The three landers will cooperate while performing acoustic and seismic experiments and will acquire different sets of measures of temperature and magnetic field at ground level.
- a high resolution map (10 m definition) of a portion of the far side. This operation will be carried out by the carrier spacecraft on a low lunar orbit and will provide information to select a possible landing site.
- a measurement of the gravitational field of the Moon.
- A Lagrangian Orbit Determination Experiment will provide information on libration points stability and perturbation environment.
- Micro Infrared Spectrometer and Radio Astronomy experiments results.

The scientific goals of the mission has strongly influenced the mission analysis design process introducing strict constraints on the possible operative orbits and their transfer trajectories. The launch is scheduled in 2015, the whole mission lasts from September 2015 till June 2017. The cooperation between orbiter and carrier requires an appropriate scheduling of mission phases according to the launching opportunities and the ideal conditions to perform the experiments.

## **2 THE SPACECRAFTS**

### **2.1 Orbiter**

The orbiter will be of the 100 kg class and will be launched as a secondary payload on an ASAP like platform or as a piggyback. The spacecraft embark the following scientific payloads:

- Micro Infrared Spectrometer (MIS) with a mass of 2.3 kg and a required input power of 4 W. It has to be continuously pointed towards the moon.
- Lagrangian Orbit Determination Experiment (LODE) with a required mass of 6.2 kg and an input power of 2 W.
- Radio Astronomy experiment (RAS). This payload requires accurate deep space pointing direction.

In addition the spacecraft will give navigation support and data relay to the net lander and will perform the carrier tracking during the Moon Gravitational Experiment, when that can not be accomplished from Earth due to the lack of visibility.

The designed satellite bus is a three axis stabilized box with a dry mass of about 75 kg and a total launch mass of about 125 kg (a margin of 10% is included).

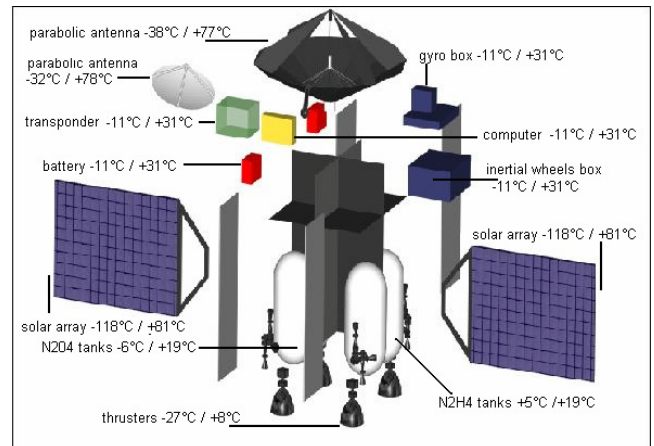


Fig. 1: Orbiter internal configuration and temperatures resulting from the thermal analysis. The first value refers to the cold case, the second to the hot case.

The main engine system is made of four bipropellant (N<sub>2</sub>O<sub>4</sub>/N<sub>2</sub>H<sub>4</sub>) chemical thrusters giving a 22 N thrust each and 308 s of specific impulse. The satellite is powered by two deployable and adjustable solar arrays with a 0.3 m<sup>2</sup> area each and 32 Li-ion cells that deliver a total bus voltage of 28 V.

Figure 1 shows the internal configuration of the satellite with the temperature values resulting from the thermal analysis.

There are 12 smaller thrusters to provide for station-keeping manoeuvres and attitude control; these devices are located on the vertexes of the main body.

The solar arrays have a 2.10 m full span and can rotate on their axis. The connection is placed in proximity of the supposed centre of mass position; they cannot be placed in an higher position not to interfere with the star trackers sensors field of view. There are four sun sensors, placed in pairs (perpendicular) on the lateral faces, and two star trackers, placed on the sun-free faces. The field of view of the star sensors (40°) is designed not to interfere with the solar arrays position and the opened high gain antenna. The sun-free faces are dedicated to the thermal radiators. The Micro Infrared Spectrometer (MIS) is placed near the antennae. The orbiter has two high gain antennae. The fixed one is a deployable parabola (0.75 m of diameter); the smaller parabola is placed on a robotic arm to maintain the link with the Earth. The orbiter has also two omni directional low gain antennae for failure recovery. The batteries are placed nearby the radiators face to dissipate excess heat and not far from the solar arrays connection. The systems boxes are placed on the structural horizontal shelf in the nearest position to the main inertial axes to reduce the momentum of inertia of the s/c.

## 2.2 Carrier

The primary aim of the carrier is to transport the three landers close to the Moon surface. In addition the carrier must perform a surface mapping and will be used as a beacon for the Moon Gravitational field experiment. The installed scientific payloads are:

- Micro High Resolution Mapping (MHRM: 1 kg - 9 W) camera for the landing site. It requires a maximum working altitude of 600 Km.
- Descent Camera (DEC). Its mass is 0.2 kg and the necessary power is 10 W.

The satellite bus is a three axis stabilized box with a triangular base pyramid on top that represents the fixing structure for the landers. The total mass is 769 kg (299 kg dry mass), considering the upper stage solid rocket (Star 48A, 78890 N thrust, 290 s specific impulse) and the orbital module the total mass at launch gets to 3169 kg. For the final Moon descent and landing phase four bipropellant (N<sub>2</sub>O<sub>4</sub>/N<sub>2</sub>H<sub>4</sub>) chemical thrusters of 556 N thrust each and 330 s of specific impulse are used while the spacecraft is powered by arrays panels for a total 1.2 m<sup>2</sup> area and by 120 Li-ion cells batteries.

Figure 2 shows the internal configuration of the satellite with the temperature values resulting from the thermal analysis.

There are 12 smaller thrusters to provide for attitude control; these devices are located on the vertexes of the main body. The solar arrays have a 2.70 m full span and can rotate on their axis. There are four sun sensors, placed in pairs (perpendicular) on the lateral faces, and two star trackers, placed on the sun-free faces; the field of view of the latter (40°) is designed not to interfere with the solar arrays position. The sun-free faces are dedicated to the thermal radiators too. The carrier has one high gain antenna placed on a robotic arm. Its diameter is of 8 cm and it is used both for link to the Earth and to the orbiter s/c. During the transfer orbit and the gravitational experiment phases the links are maintained by two omni directional low gain antennae; they work also for failure recovery. An entire face must be dedicated to the landers-supporting structure; a clear separation from the s/c after landing must be provided. The carrier solar arrays will be ejected before the deorbiting not to interfere with landers separation from the main body. The batteries are placed nearby the radiators face to dissipate excess heat and not far from the solar arrays connection. The four main thrusters are placed into the central structural cylinder; this cylinder has a base of 40 cm of radius (nearby engines) and the other of 30 cm of radius. The propellant tanks are of toroidal form, bent around the central cylinder. The shape of this tanks is the best

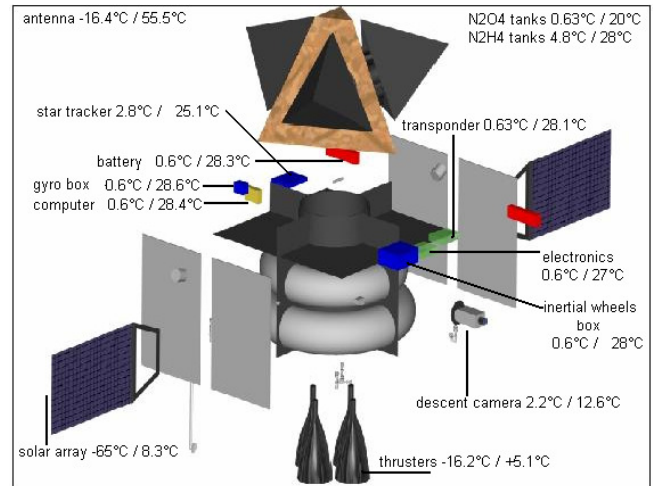


Fig. 2: Carrier internal configuration and temperatures resulting from the thermal analysis. The first value refers to the cold case, the second to the hot case.

solution for volume distribution and centre of mass position.

## 2.3 Landers

The landers provide accommodation and mounting services as well as proper thermal environment for the scientific instruments and system devices.

A petal opening system with solar arrays mounted on the internal face of each petal has been chosen. Solar arrays total surface area is 0.75 m<sup>2</sup>. Each lander is a tetrahedron and consists of a triangular base with three similar triangular side petals.

Each of the four petals is protected during the impact with the Moon surface by a 6-lobed airbag. All electronic systems are accommodated together with the thermal control subsystem in a volume on the base.

All the scientific payload are mounted on a robotic arm; these include:

- Moon Ground Acoustic experiment (MOGA: 100 g), and Micro Seismic & Surface Accelerometer Experiment (MISA: 1 kg): it will be put in direct contact with the surface of the Moon.
- Lunar Surface Temperature experiment (LST: 90 g, 0.2 W): a direct contact with the ground is required.
- Surface Magnetometer (SMAG: 100 g, 1 W): i magnetometer system for three axis measurements.

Each lander has also a camera, mounted at the top of a deployable mast, which can be used both as a panoramic camera and Micro Stereo Camera to target the robotic arm pointing. Figure 3 shows the internal configuration of the landers with the

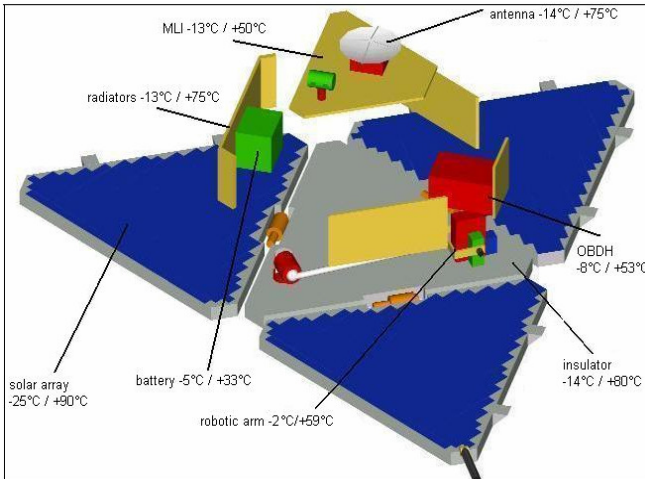


Fig. 3: Landers internal configuration and temperatures resulting from the thermal analysis. The first value refers to the cold case, the second to the hot case.

temperature values resulting from the thermal analysis.

A simple model to calculate the whole airbag system mass has been developed. The evaluation has been retro-used on the historical data of two similar airbag landing systems: Mars Pathfinder and Mars Exploration Rover; the test evaluation has been found to be correct.

The airbag is composed of 24 spherical lobes (6 per face) of 0.137 m. The internal volume of the bladder is 1.9 m<sup>3</sup>. For this volume only one gas generator (based on a solid propellant burner) is necessary to inflate the airbag to a pressure of 10600 Pa in 1.5 s and to maintain this pressure for about 20 s during the bounces on the Moon ground. The mass of the system is of about 6 kg.

### 3 MISSION ANALYSIS

#### 3.1 Orbiter

##### 3.1.1 Operative Orbit

The selection of the Orbiter Spacecraft operative orbit has been mainly driven by the necessity to create an uninterrupted communication link between the far side of the Moon and the Earth ground stations. The spacecraft has been placed on an L2 Halo Orbit since previous work by Farquhar<sup>1,2</sup> outlined the advantages of this solution with respect to relay satellites in lunar orbits.

Table 1 shows the Halo orbit main dimensions.

A <sub>x</sub>	A <sub>y</sub>	A <sub>z</sub>
23399 km	61265 km	8344 km

Table 1: Halo amplitudes of motion. The x and y axes define the Moon orbital plane with the first constantly pointing towards the celestial body.

The choice of the best target orbit for the mission, among those that satisfy the communication constraint, has been accomplished in collaboration with the Telecom and Attitude Determination and Control (ADCS) subsystems. The best compromise between manoeuvres cost, communication and pointing requirements has been investigated on the basis of the following parameters:

- Manoeuvres required to maintain a periodic motion.
- Celestial coordinates of the Moon and the Earth in the spacecraft reference frame. These coordinates are used to design the slow manoeuvre required to point toward each one of the two celestial bodies.
- Angle of the view cone including both the primaries.
- Area of coverage for each one of the two primaries.

Table 2 shows the above parameters values for the selected orbit.

$\Delta v$	0.03 m/s
Period	14.8 d
Moon Max $\Phi_y / \Phi_z$	3.9°/30.6°
Earth Max $\Phi_y / \Phi_z$	0.46°/4.4°
$\beta$ Moon	57.8°
$\beta$ Earth	84.8°
Max $\alpha$	28.7°

Table 2: Main parameters of the selected halo orbit.  $\Phi_y$  and  $\Phi_z$  are the angles of the attitude manoeuvres required to point the primaries.  $\alpha$  is the view cone angle including both the celestial bodies and  $\beta$  is the angle of the cone subtending the area that is always covered by the spacecraft.

The relatively large excursion of the spacecraft trajectory from the Lagrangian point amplifies the effects of the perturbations on the satellite's motion.

The most important effects are due to I) the eccentricity of the Earth's orbit and II) the gravitational oblateness of the Moon. Solar radiation pressure and planetary perturbations are of small significance. These perturbations must be actively balanced by station keeping manoeuvres at regular intervals during the mission lifetime.

Numerical simulations led to a total cost of 88 m/s per year for orbit maintenance.

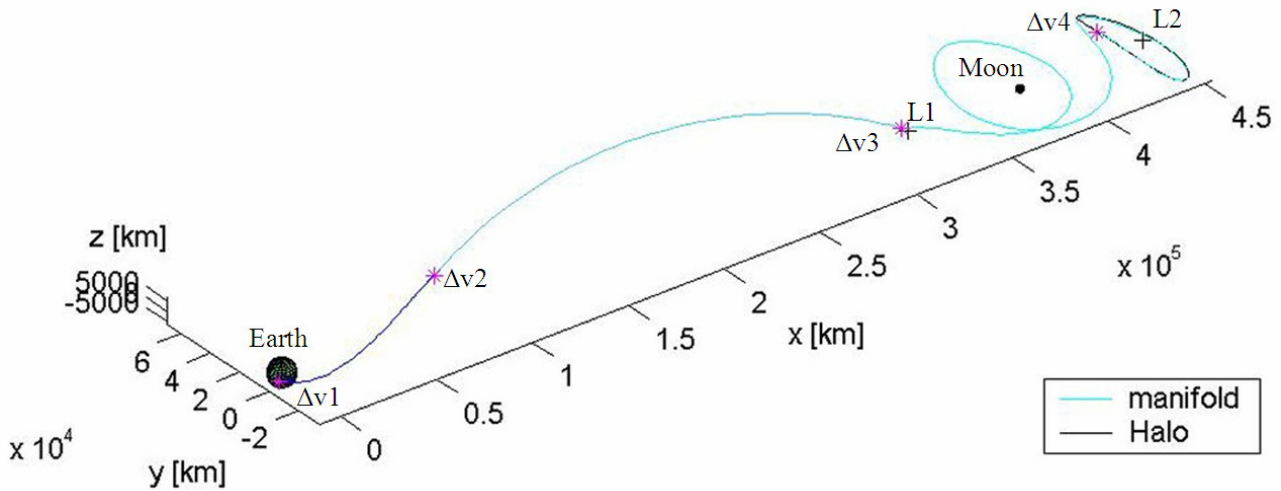


Fig. 4: Earth-L2 transfer orbit.  $\Delta v_1$  is the sum of the  $\Delta v$  to correct the parking orbit inclination and the  $\Delta v$  for the transfer injection,  $\Delta v_2$  is imposed in deep space,  $\Delta v_3$ , in proximity of the Lagrangian point L1, allows the orbiter to reach the stable manifold and  $\Delta v_4$  is the perturbation to pass from the manifold to the Halo orbit.

### 3.1.2 Transfer trajectory

Since the operative orbit is around a collinear libration point of the Earth-Moon system, a low energy optimal Earth-Halo transfer has been designed exploiting the stable and unstable manifolds of L1 and connecting them to the stable manifolds of the L2 Halo orbit. Details of the equations and problem formulation can be found in the reference<sup>9,10,11</sup>.

While it would be desirable to examine all the insertion points for an optimal trajectory, computational requirements prohibit it and only few possibilities have been analysed in this work to demonstrate the validity of the optimization method used.

Considering backward integration, the first part of the transfer orbit follows the manifold; subsequently two  $\Delta v$ s are imposed to reach a spherical corona around the Earth and, at this point, another  $\Delta v$  is necessary to obtain an elliptical orbit. The first manoeuvre (in the sense of backward integration from the insertion point) is placed close to L1 in order to exploit the peculiarities of this region to reduce the cost. The last correction  $\Delta v$  allows to reach the orbit plane, where lies the parking orbit; since optimal transfers lies in the moon orbital plane this manoeuvre turned out to be the most expensive.

The sum of all the  $\Delta v$  imposed is minimized, by genetic algorithms, that provide a first guess solution that is then refined with an SQP procedure. Figure 4 shows the transfer trajectory in the synodic reference frame.  $\Delta v$  values and trajectory segments time intervals are shown respectively in Table 3 and Table 4.

$\Delta v_1$ for transfer injection	667.0 m/s
$\Delta v_2$	0.0 m/s
$\Delta v_3$	593.4 m/s
$\Delta v_4$	0.03 m/s
Total transfer $\Delta v$	1260.43 m/s
Statistical $\Delta v$	126 m/s

Table 3:  $\Delta v$  values for the transfer trajectory.

Transfer starting time	$t_0$
Time following the first $\Delta v$	$t_0 + 0.42$ d
Time following the second $\Delta v$	$t_0 + 3.4$ d
Time on the manifold	$t_0 + 31.5$ d
Total transfer time	31.5d

Table 4: Timeline of the transfer trajectory manoeuvres.

On total  $\Delta v$  a statistical effect of perturbation has been added as a percentage (10 %) of total transfer cost; this margin comprehends a correction  $\Delta v$  for gravity losses also.

The launch vehicle selected is Ariane 5 because only this launcher permits to place the orbiter as secondary payload (microsatellite class), in terms of mass and volume. The platform used is ASAP 5, into the fairing SYLDA 5.

Ariane 5 will put the spacecraft in a GTO parking orbit: this choice allows to reduce the fuel mass.

Since the mission strategy avoids a dedicated launch in order to reduce costs, different orbit phasing studies must be performed for different launching opportunities. Indeed due to the nature of the synodic system similar transfer injection conditions represents every Moon period with slight variation caused by the change in the Moon orbital parameters (the different position of the

Sun is considered as a perturbation). An example has been studied in which the Earth's oblateness (J2 term) has been exploited to obtain a  $\Delta\omega$  change of  $3.3^\circ$  during 9.78 days (22 orbits) of permanence in GTO, avoiding so any phasing manoeuvre. According to this study the launch will occur on 28<sup>th</sup> September 2015 and the orbiter will reach the Halo orbit on 8<sup>th</sup> November 2015.

### 3.2 Carrier

#### 3.2.1 Low-Lunar Parking Orbit

The carrier operative orbit requirements derive from the ground mapping operation and the gravitational experiment.

The former requires an altitude lower than 600 Km to meet the camera resolution constraint and an inclination ideal to cover the larger portion of far side area. The latter requires an altitude lower than 500 Km to avoid high third body disturbances, an high inclination in order to allow the most complete gravitational model and must be, as much as possible, free from secular disturbances.

For these reasons a frozen orbit was chosen that offers ideal conditions for both the gravitational experiment and the far side ground mapping. The orbit parameters are listed in Table 5.

	Parameters
i	90°
r <sub>p</sub>	1838 km
e	0.03
Ω	82°
ω	-90°

Table 5: Orbital parameters of the selected frozen orbit.

A 20 spherical harmonics Konopliv' model have been used for the gravity field of the Moon and this particular frozen orbit has been selected for the following reasons:

- the polar inclination allows to cover the largest portion of far side area and to acquire a complete gravitational model.
- an height of 100 Km satisfies the payloads requirements, guarantees a low sensitivity to other bodies disturbances and is a reasonable deorbiting height.
- the eccentricity is constrained from the frozen condition: the used Konopliv model shows the existence of a frozen orbit at  $i = 90^\circ$  with the indicated eccentricity.
- the value of  $\Omega$  allows the transfer  $\Delta v$  minimization. ( $82^\circ$  from the vernal equinox direction).
- the epicentre anomaly must be  $\pm 90^\circ$  to have a frozen orbit.

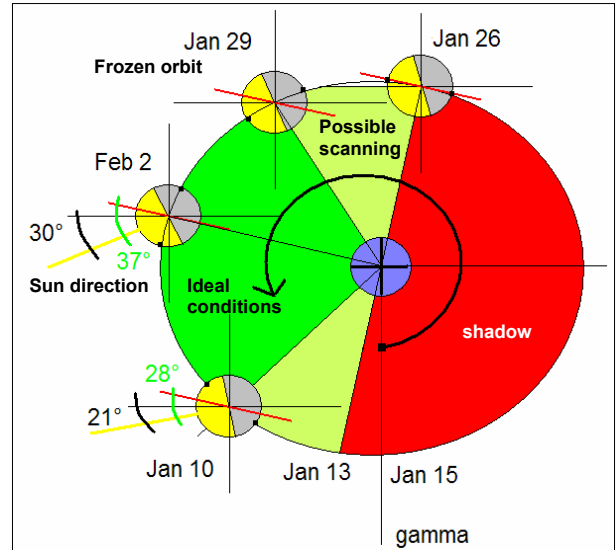


Fig. 5: Lighting condition opportunities for the scanning operation

A WSB (Weak Stability Boundaries) transfer trajectory has been design in order to insert the spacecraft in the frozen orbit on the 13<sup>th</sup> of January 2016.

Mission timeline has been properly designed in order to reach the Moon with favourable lighting conditions for the surface mapping operations.

The desired resolution is about 10 m in order to avoid all dangerous obstacles, the landing site is a 300x600 km area around the equator. The camera has two degrees of freedom and an assumed resolution of 1024x3360 pixels; it has been evaluated that the operation can be accomplished within 10 orbits. Figure 5 shows the light opportunities.

According to this analysis the mapping will be performed from the 1<sup>st</sup> to the 2<sup>nd</sup> of February while the gravitational experiment will be performed from the 3<sup>rd</sup> to the 17<sup>th</sup> of February. Deorbiting and landing are scheduled for the 28<sup>th</sup> of February.

#### 3.2.2 Earth-Moon transfer orbit

Recent studies on multi-body dynamic performed by Belbruno<sup>12,13,14</sup> have shown that if a restricted four-body problem (Earth, Moon, Sun, s/c) is considered, optimal low cost trajectories, connecting a low Earth orbit with a Moon orbit can be designed.

The point is to transit through the Weak Stability Boundary (WSB) of the Earth-Sun-Moon system, in order to obtain orbital parameters variation with a minimum manoeuvre  $\Delta v$ .

For this problem a first guess solution has been found by foreword propagation from the Earth and backward propagation from the Moon, then the result has been optimized with DITAN<sup>17</sup> satisfying the matching conditions at the WSB point. This software transcribes the equation of motion with a time finite element method and solve the resulting

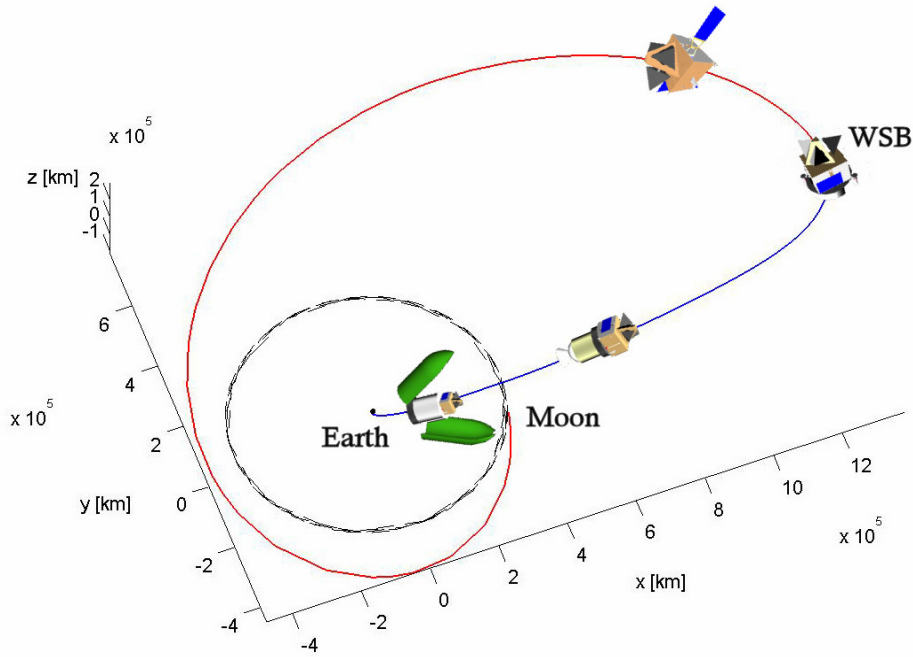


Fig. 6: First Belbruno's transfer trajectory in the Earth Equatorial system.

	First transfer	Second transfer
Departure date from LEO	25th September 2015	4th October 2015
Arrival in WSB	1st November 2015	23rd October 2015
Lunar elliptical orbit injection	13th January 2016	8th January 2016

Table 6: Belbruno's transfers opportunities.

constrained NLP problem with an SQP procedure. Two Belbruno's transfers, that satisfy the requirements, have been found (Table 6): the first one is a little more expensive than the second one, but the latter is less sensitive with respect to the initial condition. Since this type of orbit is strongly dependent from the relative position of Earth-Moon-Sun, similar launching conditions can be encountered every 6 months. Table 7 contains the needed impulses:  $\Delta v_1$  allows the Belbruno's transfer injection from LEO,  $\Delta v_2$  occurs in the WSB; after that the carrier is captured by the Moon, in an elliptical orbit, whose characteristics in an equatorial reference frame are showed in Table 8. At the pericentre,  $\Delta v_3$  is needed to circularize the orbit and finally  $\Delta v_4$  is the impulse to get into the frozen orbit.

	First Transfer	Second Transfer
$\Delta v_1$ [m/s]	3121	3073
$\Delta v_2$ [m/s]	22.1	1.0
$\Delta v_3$ [m/s]	648.2	645.5
$\Delta v_4$ [m/s]	24.3	24.3
Total $\Delta v$	3815.4	3743.8

Table 7: Manoeuvres  $\Delta v$ s for the Belbruno's transfers.

	First Transfer	Second Transfer
a [km]	39184.6	35652.3
e	0.95	0.95
i [°]	90	90
$\Omega$ [°]	84.7	82.9
$\omega$ [°]	180	36.7

Table 8: Orbital parameters of the elliptical lunar orbit in which the spacecraft is injected from the Belbruno's transfers.

The total  $\Delta v$  has been increased with a 10% margin that accounts for statistical effects of perturbation; this margin comprehends a correction  $\Delta v$  for gravity losses.

Due to its high mass, the carrier needs a dedicated launch. Dnepr-M has been selected because allows to place the carrier with an upper stage motor and an orbital module. After the launch (Baikonur, 46° N, 63° E, Kazakhstan), Dnepr will inject the carrier on a LEO parking orbit with an inclination of 63.5° and at an height of 500 km. Dnepr upper stage (Star 48A by Thiokol) provides the carrier an impulse in order to inject it on the Belbruno's transfer path. After that there is

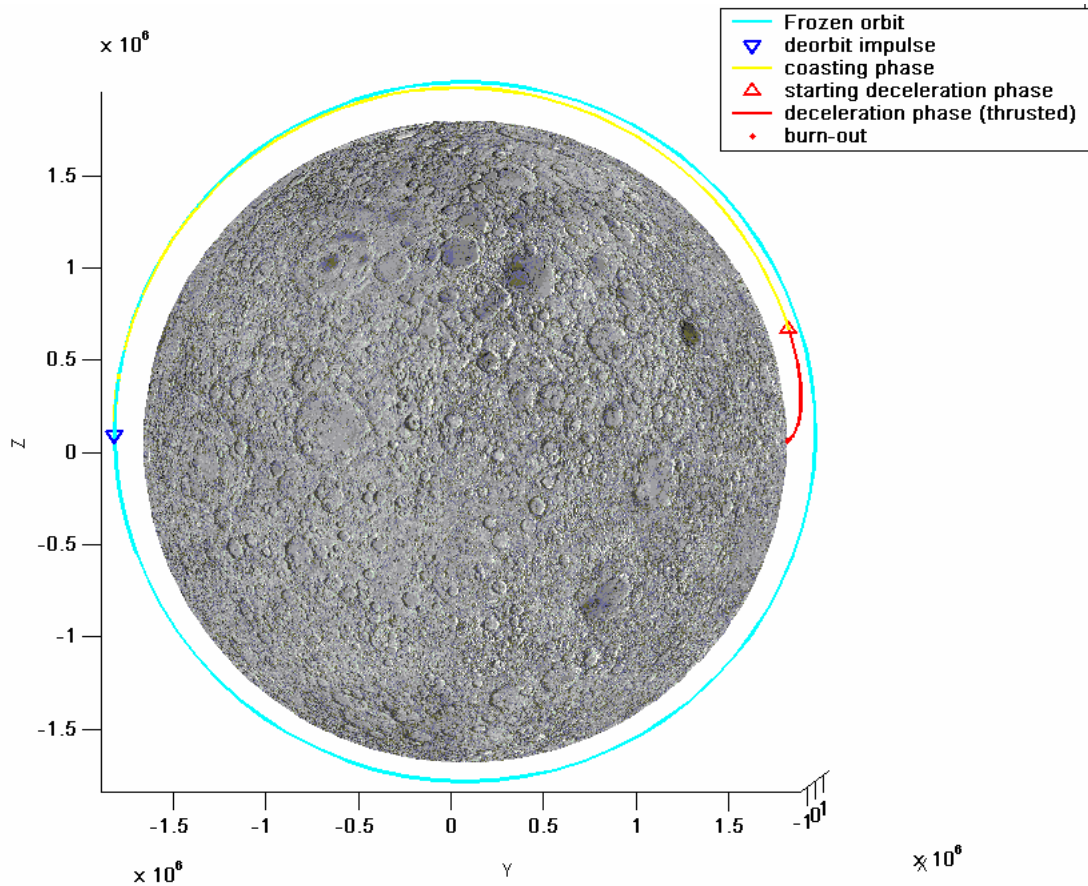


Fig. 7: On-Off-On trajectory for the deorbiting and landing phase as seen from Moon equatorial reference system.

a separation and the orbital module carries on the flight towards the WSB, where the needed impulse is given by the orbital module actuators. After the burning phase, another separation is performed and the carrier continues its path towards the Moon. The trajectory of the first transfer is shown in Figure 6.

### 3.2.3 Deorbiting and landing

After the end of the mapping operations and the gravitational experiment, the carrier waits the optimal landing conditions: best lighting and correct sub-satellite point (the plane of the orbit is fixed in an inertial Moon centred frame and the primary rotates under the carrier path).

The landers are dimensioned for a semi-hard landing at maximum acceleration of 50 g. In order to satisfy this constraint and to obtain an adequate distance between each lander on the Moon surface, the spacecraft must reach a null velocity at a maximum altitude of 35 m. This phase has been studied numerically integrating the equations of the thrust spacecraft with a variable Runge-Kutta 4/5 integrator.

The strategy adopted is an On/Off/On trajectory, designed to satisfy the following constraints:

- A coasting elliptical trajectory is designed to phase the manoeuvre with the motion of the goal area.
- The overall trajectory must have an altitude greater than 20 km in order to fly over the mountains, except for the final phase.
- The target area is a string of  $\pm 5$  km around the lunar equator.
- At the end of the last phase, the spacecraft must have burned out all the propellant in order to avoid risk of explosion during the crash. However a margin has been considered in order to target more landing zones.
- The overall manoeuvres are performed by only two of the four main engines: in case of failure it is possible to inject the other engines and continue the deceleration.

The initial conditions for the integration are the position and the velocity of the carrier on the frozen orbit and a dry mass of  $\sim 300$  kg. The resulting trajectory is characterised by a total propellant mass of  $\sim 270$  kg and a duration of 1 h 8 min 51 s for a total  $\Delta v$  of  $\sim 2080$  m/s.

Figure 7 shows the trajectory in the Moon equatorial reference system.

### 3.2.4 Impact simulation

A Working Model 3D® simulation has been developed to evaluate the landing conditions (necessary to provide data for the structure and airbag system design). The target of the simulation is to evaluate the linear and angular acceleration at the impact, the impact speed (from which derives the airbag energy absorption) and the landers bounce on the Moon surface after the impact. In this kind of simulation the deformability of the 24 airbag spheres is neglected, so the effective energy absorption is reduced in relation to the real impact; the sphere volumes overlap to recreate the typical lobe shape of the air cushion. Additionally, a restitution coefficient between the airbag and the Moon surface must be evaluated: analyzing data from the Space Shuttle COLLIDE series of experiments<sup>19,20</sup> it is clear that this coefficient never exceeds the value of 0.25-0.3. The higher this value, the lower the energy absorption. The calculation has been conducted with the value of 0.2 to provide a good safety range for the impact acceleration. The second coefficient necessary to this simulation is the coefficient of friction, it influences the body movement after the bouncing phase, before the full stop. As the correct value for this coefficient on the lunar surface has never been evaluated, the value of 0.7 has been estimated.

It is considered that the landers separate from the carrier at the height of 35 m over the ground, assuming the lander has come to a full stop in both vertical and horizontal directions. The speed vector of the lander after the separation has an inclination of 60° over the horizontal plane; the speed is 5 m/s, and the ejection is provided by a spring device.

The study of the angular acceleration has been neglected because the linear one is quite more relevant for the evaluation of the structure stresses. The simulations showed that the acceleration do not exceed 45 g. The structure analysis will be conducted on the value of 50 g to provide a range of safety. Impact velocities remain below 15 m/s, so the airbag must be designed to absorb an energy of about 4000 J. The stop distance estimated is about 100 m from the first impact point.

### 3.3 Eclipses analysis

Eclipse determination procedure was based on the reciprocal position of Sun, Earth and Moon and their apparent radius in relation with the spacecraft position.

The analysis leads to the following conclusions:

- Orbiter: During the transfer trajectory of the orbiter only one partial eclipse was found and due to Earth. It is only 10 min long. On the Halo orbit around L2 only one eclipse was

found and it is 85 min long (62 min of total eclipse). The event takes place the 24th of February 2016.

- Carrier: During the transfer trajectory of the carrier any relevant eclipses were found. On the frozen orbit around Moon several eclipse phenomena were found. The orbital period of the carrier is 2 h and every revolution the spacecraft experiences a Sun occultation (caused by the Moon) that varies from 26 to 48 min depending on the day.
- Landers: Landers last in Moon shade for 14.6 d every Moon revolution period.

No limitation on the orbiter mission planning resulted from the previous analysis, according to the power and thermal studies. The shading periods on the orbiter are few and their length is negligible. Different conditions were found for the carrier.

It will experience several cycles of night and day and will have only 1.11 ÷ 1.33 h of lighting every frozen period.

The landers conditions are extremely severe (14.6 d every Moon revolution period) and their design and operational planning will be enslaved to that. Figure 9 shows the night and day cycles for the three landers during the year 2016.

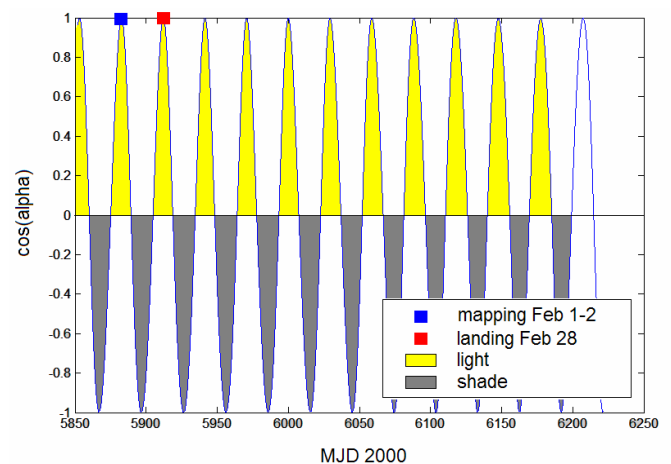


Fig. 9: Lighting conditions of the landing site for the year 2016. The highlighted points represent the carrier mapping operations period and the landing phase.  $\cos(\alpha) = 1$  corresponds to the optimal illumination conditions, when the sun vector is parallel to the landing site local normal.

### CONCLUSIONS

The result of this mission design process is a low cost mission that could work as a path finder for bigger far side lunar programs. The mission indeed contemplates a complex scientific program whose results will be useful for either the establishment of a lunar base, the placement of permanent scientific facilities or the creation of a

lunar communication bridge with the outer space. Important information can be obtained from the data of the net-lander and its behaviour during the night and day cycles, and from the orbiter satellite on the Halo orbit.

A further phase A study will need to address in more detail the following aspects:

- A finer analyses of the launch windows.
- Orbit determination and navigation analysis.
- Failure analyses of the orbit injections.
- Orbit maintenance manoeuvres schedule.
- Ground segment design.

### ACKNOWLEDGEMENT

The mission "Hevelius" is a pre-phase A study designed at the "Politecnico di Milano" from a group of students during the class of "Space System Design" and with the supervision of Prof. Massimiliano Vasile.

The authors would like to thank the other students and everybody that contributed to the realization of the project with his work or his help.

A copy of the report can be asked to the authors or at the Aerospace Department of the "Politecnico di Milano".

### REFERENCES

1. Farquar, R. W., "Future Missions for Libration-point Satellites" *Astronautics & Aeronautics*, Vol. 7, No. 5. 1969.
2. Farquar, R. W., "Lunar Communications with Libration-Point Satellites." *Journal of Spacecraft Rockets*, Vol. 4, No. 10, Oct. 1967.
3. Schmid, P. W., "Lunar Far-Side Communication Satellites," NASA, TN D-4509, June 1968.
4. Farquhar, R. W., D. P. Muhonen, C. R. Newman, and H. S. Heuberger, "Trajectories and Orbital Maneuvers for the First Libration-Point Datellite. " *Journal of Guidance and Control*, Vol. 3, No. 6, November-December 1980..
5. Richardson, D. L., "Analytic Construction of Periodic Orbits About the Collinear Points," *Celestial Mechanics* 22 (1980) 241-253.
6. Richardson, D. L., "Halo Orbit Formulation for the ISEE-3 Mission," *Journal of Guidance and Control*, Vol. 3, No. 6, November-December 1980.
7. Howell, K. C., D. L. Mains, and B. T. Barden, "Transfer Trajectories From Earth Parking Orbits to Sun -Earth Halo Orbits," AAS-94-160, AAS/AIAA Spaceflight Mechanics Meeting, Cocoa Beach, FL, February 14-16, 1994.
8. Gómez, G., A. Jorba, J. Masdemont, and C. Simò [1991], " Study Refinement of Semi-Analytical Halo Orbit Theory," Final Report, ESOC Contract No.: 8625/89/D/MD(SC), Barcelona, April, 1991.
9. Koon, W.S., M.W. Lo, J.E. Marsden and S.D. Ross [2000b], "Shoot The Moon", AAS/AIAA Astrodynamic Specialist Conference, Florida, 2000, AAS 00-166.
10. Lo, M. and S. Ross [1998] "Low energy interplanetary transfers using invariant manifolds of L1, L2 and halo orbits," AAS/AIAA Space Flight Mechanics Meeting, Monterey, California, 9-11 February 1998.
11. Starchville, T. F. and R. G. Melton, "Optimal Low-Thrust Trajectories to Earth-Moon L2 Halo Orbits (Circular Problem)" AAS/AIAA Astrodynamics Specialist Conference, Sun Valley, ID, August 4-7, paper no. AAS 97-714.
12. Belbruno E. A., "Lunar capture Orbits, a Method of Constructing Earth-Moon trajectories and The Lunar GAS Mission", AIAA, 87-1054.
13. Belbruno E. A., Miller J. K., "Sun-Perturbed Earth-To-Moon Transfers With Ballistic Capture", *Journal of Guidance Control, and Dynamics*.
14. Belbruno E. A., Humble R., Coil J., "Ballistic Capture Lunar Transfer determination for the US Air Force Academy Blue Moon Mission", AAS, 97-171.
15. Comoretto G., Ercoli Finzi A., Vasile M., "Ottimizzazione di trasferimenti WSB Tramite Combinazione di Metodi Euristici e Sottoprogrammazione Quadratica", 2000.
16. Whitcomb, G.P., "The ESA approach to low-cost planetary missions", *Acta Astronautica* 52 (2003) 79-86.
17. Vasile M., Bernelli-Zazzera F., Fornasari N., Masarati P. "Design of Interplanetary nad Lunar Missions Combinino Low Thrust and Gravity Assists". Final Report of ESA/ESOC Study Contract No. 14126/00/D/CS, ESA/ESOC.
18. Wertz J. R., Larson W. J., *Space Mission Analysis and Design*, 3rd edition, Microcosm Press, California, 1999.
19. Doengi F., Burnage S. T., Cottard H., Roumeas R., "Lander Shock-Alleviation Techniques", *ESA Bulletin*, February 1998.
20. Doengi F., Burnage S. T., Cottard H., Roumeas R., "Lander Shock-Alleviation Techniques", *Esa Bulletin*, n. 93, Feb 2000.